LANGEVIN SIMULATION OF RF CORONA DISCHARGES FOR SPACE HARDWARE

M. Alfonseca[(1)], L. Conde[(2)], J. de Lara[(1)], F. Pérez[(1)], D. Raboso[(3)]

[(1)] Escuela Técnica Superior de Informática, Universidad Autónoma de Madrid
Francisco Tomás y Valiente 11, 28049-Madrid, Spain
Email: {francisco.perez, juan.delara, manuel.alfonseca}@uam.es

[(2)] Departamento de Física, E.T.S.I. Aeronáuticos, Universidad Politécnica de Madrid
28040-Madrid, Spain
Email: lconde@faia.upm.es

[(3)] ESA/ ESTEC
Keplerlaan 1, 2200 AG Noordwijk, The Netherlands
Email: david.raboso@esa.int

ABSTRACT

The corona effect in space radio frequency (RF) hardware is an electric breakdown process at low neutral gas pressures originated by the progressive outgassing of the entire RF system. A small number of seeding electrons are accelerated by the RF electric field and their subsequent inelastic collisions with neutral atoms and ionizations produce the multiplication of charges in the gap between the conducting walls of the RF system. The simulation of the early stages of the corona effect is performed through the numerical integration of the individual trajectories of the electrons in a simplified model of a waveguide made of infinite parallel metallic walls. The electron dynamics is described by dimensionless Langevin equations, where the RF field is the deterministic driving force and an additional stochastic force term describes the interaction between the electrons and the neutral gas background. The charge multiplication process is caused by the electron impact ionization of the neutral atoms and the secondary electron emission at the walls of the waveguide. The physical properties of different materials for the walls of the waveguide are also taken into account. We present the basis of the model and the characteristics of the numerical integration scheme, as well as the physical conditions under which charge multiplication develops. The limitations of the proposed model, as well as the current limitations in the available experimental data, are also discussed.

1. INTRODUCTION

The corona effect in space RF hardware can be defined as a local electric discharge initiated by gas ionization. This electric breakdown requires neutral gas pressures lower than ground levels, caused by the progressive outgassing of the entire RF system with the increasing altitude reached by the spacecraft. The corona effect typically develops at altitudes between 60 and 80 Km, when the Telemetry, Tracking and Command subsystem inside communications satellites is switched on [4]. This electric discharge takes place under sharply non-uniform electric fields and is initiated by a very small number of electric charges (mainly electrons), as low as 10^{-14}A [11]. The origin of such low currents is the everywhere present cosmic rays or natural radioactivity, leading to corona being classified in the group of *self sustained discharges* [3][11]. These seeding charges are accelerated by the RF electric field and their subsequent elastic collisions with neutral atoms and ionizations produce the multiplication of charges in the gap between conducting walls.

The involved neutral gas pressures in corona discharge are several orders of magnitude higher that in multipactor (MP) or high vacuum electric discharges. In consequence, the collisional mean free paths ($?_{ea}$ for elastic collisions between electrons and neutral atoms and $?_I$ for ionizations) are shorter than the typical waveguides gap sizes. In addition, the corresponding ionization frequencies ($?_{ea}$ and $?_I$) are larger than those of external RF signal frequencies. These collisional processes introduce additional length and time scales and relevant differences from previous work with multipactor electric discharge.

In this work we formulate a simplified physical model in three dimensions, intended to simulate the charged particle multiplication of corona discharge. The numerical simulations considers the simplified waveguide model of Fig. 1, composed of two parallel metallic walls (which will also be called *electrodes* in the following) where a sinusoidal high voltage electric field exists. In the inter-electrode space, a low pressure of different neutral gases is considered in the simulations.

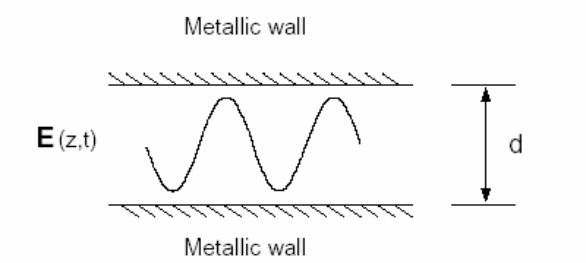

Fig. 1. Scheme of the model for the waveguide, with the electric field *E(z, t)* perpendicular to the parallel walls.

For the involved neutral gas pressures, the description of the interaction between the huge number of neutral atoms (n_a ~ 10^{17} cm^{-3}) and a relative small number of electrons is a hopeless task. Then, the electrons will be considered as immersed in a neutral gas atom background moving under averaged approximated forces and the RF electric field. The random elastic collisions with neutral atoms scatter the negative charges from their original directions, which are modelled by means of a fluctuating random force, coupling the three directions of motion. Then, electrons move in a three dimensional random walk under a deterministic RF driving electric force. Their trajectories in the inter-electrode gap are obtained by the numerical integration of the stochastic equations of motion. Similar models using Langevin equations have been proposed to study high pressure multipactor discharge [6][12][14][15][16][17] as well as the dynamic of charged particle beams [9][10].

2. MODEL EQUATIONS

In the present model, the charge multiplication processes in the waveguide are simulated following the individual time evolution of a small number of electrons. Initial seeding electrons are randomly distributed in one of the plates, at the first wave of the RF electric field. Additional electrons are produced by electron ionization impact of the neutral gas, and also at the walls of the waveguide by secondary emission. The charged particles may be lost when they move away from the simulation volume, or are absorbed by the waveguide walls when the electron energy is negligible. The volume recombination and/or electron attachment are neglected, because the corresponding average free paths exceed the dimensions of typical waveguide sizes.

The charge multiplication process is considered to take place at the time when the ratio between the number of electrons present in the waveguide gap and the initial electrons lies over a critical threshold. In consequence, during the simulation, the number of electrons and ions remain very small compared with the huge quantity of neutral atoms. The local electric field created by charged particles is therefore screened and small compared with the externally imposed RF electric field. Thus, the charge space effect will be not considered, as in previous models [6][12][14][15][16][17]. Finally, the energy imparted by the external RF electric field between two successive collision events is larger than all collisional energy losses.

2.1. Electron Trajectory

The motion of each individual electron is determined by the deterministic RF electric force $F_e = -e \cdot E(t)$ along the perpendicular axis (*Z*), and by its interaction with the neutral atom background, which considers an averaged friction force $F_r = -m_e \cdot ?_m \cdot v_e$ along each direction. The elastic collisions with neutrals which scatter the electrons are described by means of fluctuating random forces along each direction:

$$F_{xr} = \sqrt{C_x}\, z_x(t)$$
$$F_{yr} = \sqrt{C_y}\, z_y(t)$$
$$F_{zr} = \sqrt{C_z}\, z_z(t)$$

Because the neutral atom density is constant, these coefficients have the same value $C_x = C_y = C_z = C$ and are constant along the inter-electrode gap. The Langevin equations of motion for electrons are,

$$\frac{dr_e}{dt} = v_e$$
$$m_e \frac{dv_e}{dt} = -eE(t) - m_e u_m v_e + \sqrt{C}z(t) \quad (1)$$

where *?(t)* is the gaussian additive random white noise, which satisfies,

$$< z(t) > = 0$$
$$< z_i(t) z_j(t') > = d_{ij} d(t - t')$$

where the symbol < … > indicates ensemble average. As in [9][10], constant *C* is,

$$\sqrt{C} = m_e \sqrt{u_m} \sqrt{\frac{2K_B T_e}{m_e}}$$

which is also related with the energy dissipation and satisfies the right units in (1).

Equations in (1) are made dimensionless with the RF signal frequency *f* as time scale $t = t \cdot f$ and the waveguide gap *d* for longitudes. In consequence we introduce, $r_x = x/d$, $r_y = y/d$ and $r_z = z/d$ and the normalized speeds,

$$\frac{dr_x}{dt} = U_{r_x} = \frac{V_x}{fd}$$
$$\frac{dr_y}{dt} = U_{r_y} = \frac{V_y}{fd}$$
$$\frac{dr_z}{dt} = U_{r_z} = \frac{V_z}{fd}$$

The following dimensionless equations are deduced from (1),

$$\frac{dU_{r_x}}{dt} = -\frac{u_m}{f} U_{r_x} + \frac{V_{eT}}{df} \frac{u_m}{f} z_x(t)$$
$$\frac{dU_{r_y}}{dt} = -\frac{u_m}{f} U_{r_y} + \frac{V_{eT}}{df} \frac{u_m}{f} z_y(t) \quad (2)$$
$$\frac{dU_{r_z}}{dt} = -\frac{u_m}{f} U_{r_z} - \frac{1}{2}\left(\frac{V_{me}}{df}\right)^2 \sin(2pt) + \frac{V_{eT}}{df} \frac{u_m}{f} z_z(t)$$

where V_{me} is the maximum electron velocity.

The limits of the current model are determined by the dimensionless coefficients in (2) which essentially consider the thermal spread of initial electrons, the effective elastic collision frequency and the RF electric field. The trajectories of individual electrons are obtained by the integration of (2) and a typical trajectory is shown in Fig. 2, where the effect of the random component of the movement equations is not as evident as in Fig. 3, due to a very low gas pressure (0.1 Torr) and a small waveguide gap (1 mm). The effect of the initial energy spread of electrons is also shown in Fig. 3.

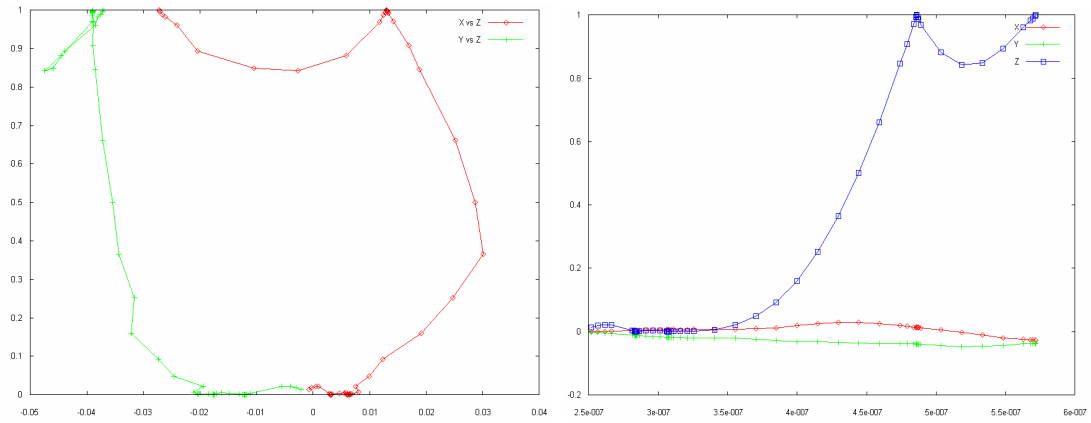

(a) (b)

Fig. 2. (a) Typical trajectory of an electron in the xz (red) and yz (green) planes of the numerical simulation, and (b) x,y, z coordinates of its position with respect to time.

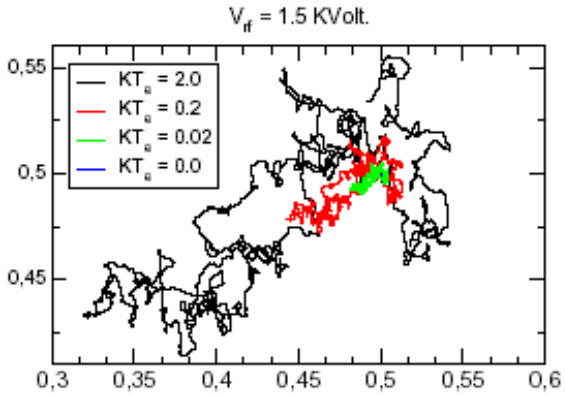

Fig. 3. Effect of the energy spread $K_B T_e$ in the numerical simulations.

2.2. Ionization collisions

The model for the motion of the electrons exposed above has considered the effects of the elastic collisions between the electron and the atoms, as well as the influence of the Z-axis force, due to the RF electric field, but not the way of introducing new electrons by the ionization of the neutral gas.

In order to determine the number of ionizations in the neutral gas, more concretely, the instant of time in which new electrons are created, the free path cover for the electron L and the ionization energy E_I of the atoms in the neutral gas are considered. Statistically, we know that the collisional mean free path for ionizations $?_I$ is the average distance that an electron must cover to produce ionization. Thus, one new additional electron is introduced when both $L > ?_I$ and the electron energy exceed the ionization threshold E_I. Fig. 4 shows how new electrons are produced by ionization.

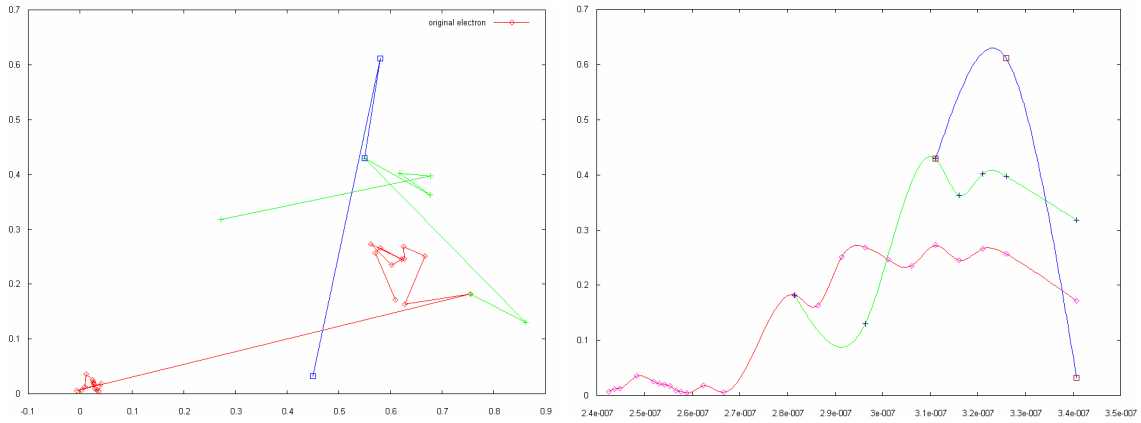

(a) (b)

Fig.4. (a) Trajectory of an electron in the xz plane, and (b) z-coordinate of its position with respect to time.

2.3. Wall collisions

When an electron collides with one of the plates, it can be absorbed; elastically or inelastically backscattered; or a number of true secondary electrons may be generated. The three kinds of emitted electrons provide their own contributions to the Secondary Electron Yield (SEY) curve, which is a function of the impacting energy (E_p) and the incidence electron angle (φ). The addition of the three contributions results in the total SEY, which also depends on the material and on surface finish properties, such as air contamination, cleanliness or surface treatments. The SEY value for an impact at a certain energy and angle gives the average number of generated electrons. Fig. 5 shows a typical SEY curve for a normal incidence angle. This curve is usually modelled by three magnitudes: E_1 and E_2 are the energies when the SEY is one, E_{max} is the energy when the SEY gets its maximum value. We use a model with more refined parameters set, resulting from fitting experimental data for many materials, either from our experimental data or from the literature.

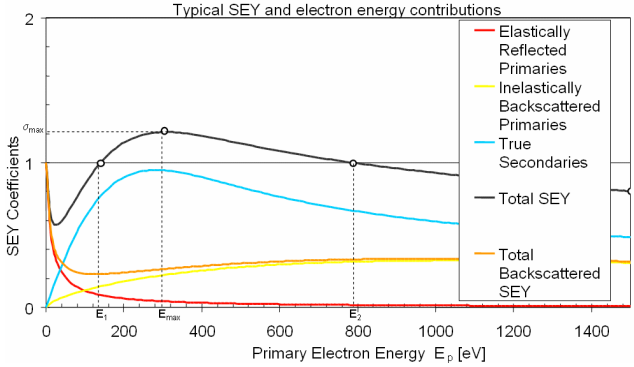

Fig. 5. A Typical SEY curve.

The total SEY (s), is modelled as the sum of the contribution of inelastically backscattered electrons (h), elastically backscattered electrons (e), and true secondary electrons (d): $s(E_p) = h(E_p) + e(E_p) + d(E_p)$, where e, d and h are dependant on material properties, in particular h depends also on the atomic number of the coating material. Additionally, we have to take into account the angle j with which the electron collides. This can be separately modelled as for each type of collision. In this way, the final SEY has an expression like the following: $s(E_p, j) = h(E_p, j) + e(E_p, j) + d(E_p, j)$. The output electron emission angles are also calculated. We consider emission angles q, with respect to the inward normal to the xy plane, and z in the xy plane. If the output electron is elastically or inelastically backscattered, its output angles are the same as its input angles (it is perfectly reflected). In the case of a true secondary electron, the angles are calculated using the cosine law distribution.

The simulation of secondary emission in wall collisions is the basis of our simulation for the prediction of the multipactor effect, and has been described elsewhere in more detail [7][8].

3. STRUCTURE OF THE SIMULATION

The corona simulator performs individual simulations for each electron, but carries a simultaneous simulation of all the electrons at the same simulation time. Each electron is represented by an object [2], with its current state, its past state, and the covered free path since its last ionization. The state consists of the position, the velocity and the time when the former values are valid for the electron. With a hybrid simulation approach [13], each entity is assessed in the next continuous simulation step, by checking that its integrity and consistency constraints are correct. The new state values may trigger a new instantaneous event, which can be an ionization or a wall collision.

In this simulation approach, a part of the system has continuous behaviour, which is perturbed by events. These can be either state events (the event depends on certain expressions of state variables) or time events (the event is scheduled to occur at a certain time). State events may occur between two time intervals of the integration method. Algorithms for efficient state location have been proposed in [1]. In any case, an abrupt variation of the state variables may occur or even the governing equations may change (mode transition).

The simulation proceeds as follows: in a first step, a number of seeding electrons are randomly distributed in an electrode. To guarantee the random initialization, they start with a normally distributed energy at a fixed point in a plate and at a uniform distributed time in the first period of the RF electric field. When the simulation time reaches an electron initialization time, a wall collision is performed for that electron.

Next, equations in (2) are integrated over a time step by using a Milstein integration scheme [5] for stochastic differential equations. The simulation processes all the electrons simultaneously, so for each electron a stochastical integration step is performed. When the final state of an electron is not consistent (its position is outside the allowed Z-range), the length step is broken in shorter time intervals and the integration step is attempted again. This usually denotes that a state event – a wall collision – should be tested for in a previous simulation time than the current time. Thus, this time should be conveniently located.

After one electron comes to a new stable state, the simulator determines whether this electron may generate a new ionization electron, by comparing the distance it has covered with the ionization mean free path of the neutral gas. The result of the ionization collision is a new generated electron without initial energy, located at the same point as the ionizing electron. The energy of the latter diminishes by the ionization energy E_I, thus preserving the energy conservation law, while the new generated electron comes under the influence of the RF electric field.

The production of additional charges by electrons that impact the waveguide walls is performed as in our multipactor simulator [7][8].

This iterative process evolves in time, and the electron avalanche is considered to occur when the number of electrons in the waveguide goes above k times the original number of seeding electrons. In a similar way, the simulation stops with a negative prediction of the corona effect when the number of electrons becomes k times less than the original number of electrons. The value of constant k may be set for each individual simulation.

4. CONCLUSIONS

In this work we have presented a model of the prediction of Corona discharge in a parallel plates geometry. The model is based on the tracking of individual electrons, following an object-oriented approach. Each electron follows a trajectory, described as a stochastical differential equation. The simulation follows a hybrid approach, and electrons may produce two kinds of state events: ionizations or wall collisions. We are currently working on the user interface of the simulator and are in the process of validating the simulator results with experimental data.

REFERENCES

[1] P.I. Barton and T. Park, 1996. "*State Event Location in Differential-Algebraic Models*", ACM Transactions on Modelling and Computer Simulation, vol. 6, no. 2, pp. 137-165.

[2] G. Booch. "*Object Oriented Design*". Benjamin-Cummings, 1991.

[3] S.C. Brown, "*Basic data of plasma physics: The fundamental data on electrical discharges in gases*". American Vacuum Society Classics American Institute of Physics, New York, (1994).

[4] J-P. Catani and J. Puech, *"Microwave breakdown in space RF hardware"*, Proceedings of the workshop on Multipactor, RF and DC Corona and passive intermodulation in space RF hardware, pp. 25-30, WPP-178, ESTEC, ESA, Noordwijk, The Netherlands. 4-6 September 2000.

[5] D.J. Higham, *"An Algoritmic introuduction to numerical simulation of stochastic differential equations"*, SIAM Review, 43, (3), pp. 525-546, (2001).

[6] A. Kryazhev, M. Buyanova, V. Semenov, D. Anderson, M. Lisak, J. Puech, L. Lapierre, and J. Sombrin, *"Hybrid resonant modes of two-sided multipactor and transition to the polyphase regime"*. Phys. Plasmas, 9, (11), pp. 4736-4743, (2002).

[7] J. de Lara, F. Pérez, M. Alfonseca, L. Galán and D. Raboso, *"Multipactor Electron Simulation Tool (MEST)"*, Proc. 26th IEEE Int. Power Modulator Symposium and 2004 High Voltage Workshop, pp.: 547-550

[8] F. Pérez, J. de Lara, J., L. Galán, M. Alfonseca, I. Montero, E. Román and D. Raboso, *"Simulation of Multipactor Effect through the Individual Simulation of Electrons"*. Mulcopim'2005 (this conference).

[9] J. Qiang and S. Habib, *"A second order stochastic leap-frog algorithm for Langevin simulation"*, Proceedings of the XX Linac Conference, pp. 89-91, Monterrey, California USA. August 21-25, (2000).

[10] J. Qiang and S. Habib, *"A second order stochastic leap-frog algorithm for multiplicative noise brownian motion"*, Phys. Rev. E, 62, (5), pp. 7430-7437, (2000).

[11] Y.P. Raizer, *"Gas discharge physics"*. Springer Verlag, Berlin, (1991).

[12] S. Riyopoulos, *"Collisional multipactor inside ambient gas"*, Phys. Plasmas, 11, (5), pp. 2036-2045, (2004).

[13] A. van der Schaft and H. Schumacher. 2000. "*An Introduction to Hybrid Dynamical Systems*". Lecture Notes in Control and Information Sciences 251. Springer.

[14] V. Semenov and A. Kryazhev, D. Anderson and M. Lisak, *"Multipactor suppression in amplitude modulated radio frequency fields"*, Phys. Plasmas, 8, (11), pp. 5034-5039, (2001).

[15] R. Udiljack, D. Anderson, M. lisak, V.E. Semenov and J. Puech, *"Multipactor in low pressure gas"*, Phys. Plasmas, 10, (10), pp. 4105-4111, (2003).

[16] R. Udiljack, D. Anderson, M. lisak, V.E. Semenov and J. Puech, *"Improved multipactor in low pressure gas"*, Phys. Plasmas, 11, (11), pp. 5022-5031, (2004).

[17] J.R.M. Vaugham. *"Multipactor"*. IEEE Trans. on Electron Dev., 35, (7), pp. 1172-1180, (1988).